Available online at www.sciencedirect.com
SCIENCE DIRECT®
Tetrahedron: Asymmetry
Tetrahedron: *Asymmetry* 16 (2005) 2653–2663

Determination of absolute configuration using vibrational circular dichroism spectroscopy: phenyl glycidic acid derivatives obtained via asymmetric epoxidation using oxone and a keto bile acid

Frank J. Devlin,[a] Philip J. Stephens[a,*] and Olga Bortolini[b]

[a]*Department of Chemistry, University of Southern California, Los Angeles, CA 90089-0482, USA*
[b]*Dipartimento di Chimica, Università di Calabria, Via Bucci cubo 12 C, 87036 Rende (CS), Italy*

Received 13 June 2005; accepted 24 June 2005

Abstract—The (+)-enantiomers of the *o*-Br, *m*-F and *p*-CH_3 derivatives of *trans* phenyl glycidic acid have been obtained from the corresponding *trans* cinnamic acid derivatives using Oxone and the *tri*-keto bile acid dehydrocholic acid. Vibrational circular dichroism (VCD) spectroscopy of their methyl esters has been used to determine their absolute configurations. In each case, the absolute configurations of both methyl ester and parent acid were shown to be (2*S*,3*R*)-(+)/(2*R*,3*S*)-(−).

1. Introduction

Bortolini et al. have shown that the asymmetric epoxidation of *trans*-cinnamic acid derivatives, using dioxiranes generated in situ from keto bile acids and potassium monoperoxy-sulfate ($KHSO_5$, Oxone), can yield *trans*-phenyl glycidic acid derivatives in high enantiomeric excess (ee).[1,2] Initial studies employed the *tri*-keto bile acid dehydrocholic acid.[1] Subsequently, a wide variety of *mono*-, *di*- and *tri*-keto bile acids were studied in order to define the roles played by the C3, C7 and C12 substituents and their optimum combination in yielding products of high ee.[2] Very recently, it has also been shown that keto bile acids can be used for the enantioselective epoxidation of unfunctionalized olefins.[3]

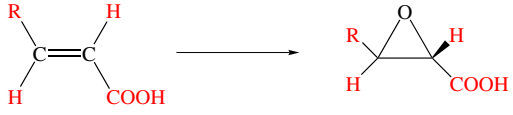

The absolute configurations of the optically active *trans*-phenylglycidic acid derivatives obtained from *trans*-cinnamic acid derivatives[1,2] had not been previously determined, with the exception of unsubstituted *trans*-phenyl glycidic acid.[4] In order to assist the elucidation of the stereochemistry of keto bile acid catalyzed asymmetric epoxidation, we undertook the determination of the absolute configurations of the methyl esters of three *trans*-phenylglycidic acid derivatives, **1**–**3**:

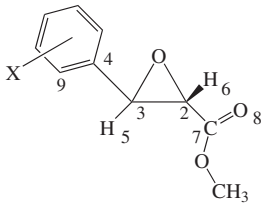

1 X =o-Br
2 X = p-CH_3
3 X = m-F

Initially, we compared the experimental specific rotations to values calculated using Time-Dependent Density Functional Theory (TDDFT) methods,[5] and concluded that the absolute configurations of **1**–**3** were all (2*S*,3*R*)-(+)/(2*R*,3*S*)-(−).[6] However, the specific rotations of **1**–**3** are relatively small and TDDFT calculations are not infallible.[7] We have therefore carried out further studies of the absolute configurations of **1**–**3** using Vibrational Circular Dichroism (VCD) spectroscopy,[8] a much more reliable technique for the determination of absolute configurations.[9–15] Herein, we

* Corresponding author. Tel.: +1 213 740 4119; fax: +1 213 740 3972; e-mail: pstephen@usc.edu

0957-4166/$ - see front matter © 2005 Elsevier Ltd. All rights reserved.
doi:10.1016/j.tetasy.2005.06.035

report our VCD studies and the absolute configurations determined.

2. Methods

IR and VCD spectra were measured for CCl_4 solutions of (+)-**1**, (+)-**2** and (+)-**3** using Nicolet MX-1 and Bomem/BioTools Chiral*IR* spectrometers, respectively. Resolutions were 1 cm^{-1} for IR spectra and 4 cm^{-1} for VCD spectra. VCD collection time was 1 h. VCD baselines were the VCD spectra of CCl_4 solutions of racemic **1**–**3**, of identical concentrations to the solutions of the corresponding optically active samples.

DFT calculations were carried out using GAUSSIAN 98.[16] Functionals were B3LYP and B3PW91, basis sets were 6-31G* and TZ2P.[9–15,17] Harmonic rotational strengths were calculated using Gauge-Invariant (Including) Atomic Orbitals (GIAOs).[18,19] Harmonic vibrational frequencies, dipole strengths and rotational strengths were converted to IR and VCD spectra using Lorentzian line shapes,[20,21] with $\gamma = 4.0\ cm^{-1}$.

Table 1. Experimental specific rotations and ees of **1**–**3**[a]

	$[\alpha]_D^{25}$	ee (%)
1	+23 (*c* 5.6, CCl_4)	46
2	+174 (*c* 4.3, CCl_4)	79
3	+154 (*c* 4.5, CCl_4)	53

[a] $[\alpha]_D$ values are corrected to 100% ee.

3. Results

The methyl esters of the *o*-Br, *p*-CH_3 and *m*-F derivatives of *trans*-phenylglycidic acid, **1**–**3**, were synthesized as described previously.[1] Their specific rotations in CCl_4 and their enantiomeric excesses (ee), determined using gas chromatography,[1] are shown in Table 1. All three compounds have positive $[\alpha]_D$ values, as do the three parent acids. Racemic forms of **1**–**3** were synthesized using Oxone in the presence of trifluoroacetone.[22]

The IR and VCD spectra of CCl_4 solutions of **1**–**3** were measured in the mid-IR spectral region, with the results shown in Figures 1–3. Baselines for the VCD spectra of solutions of (+)-**1**, (+)-**2** and (+)-**3** were provided by solutions of the same concentration of the corresponding racemic compounds. VCD spectra are corrected to 100% ee. The signal-to-noise ratios of the VCD spectra of **1** and **3** are significantly lower than that of the VCD spectrum of **2** as a result of their substantially lower ee values.

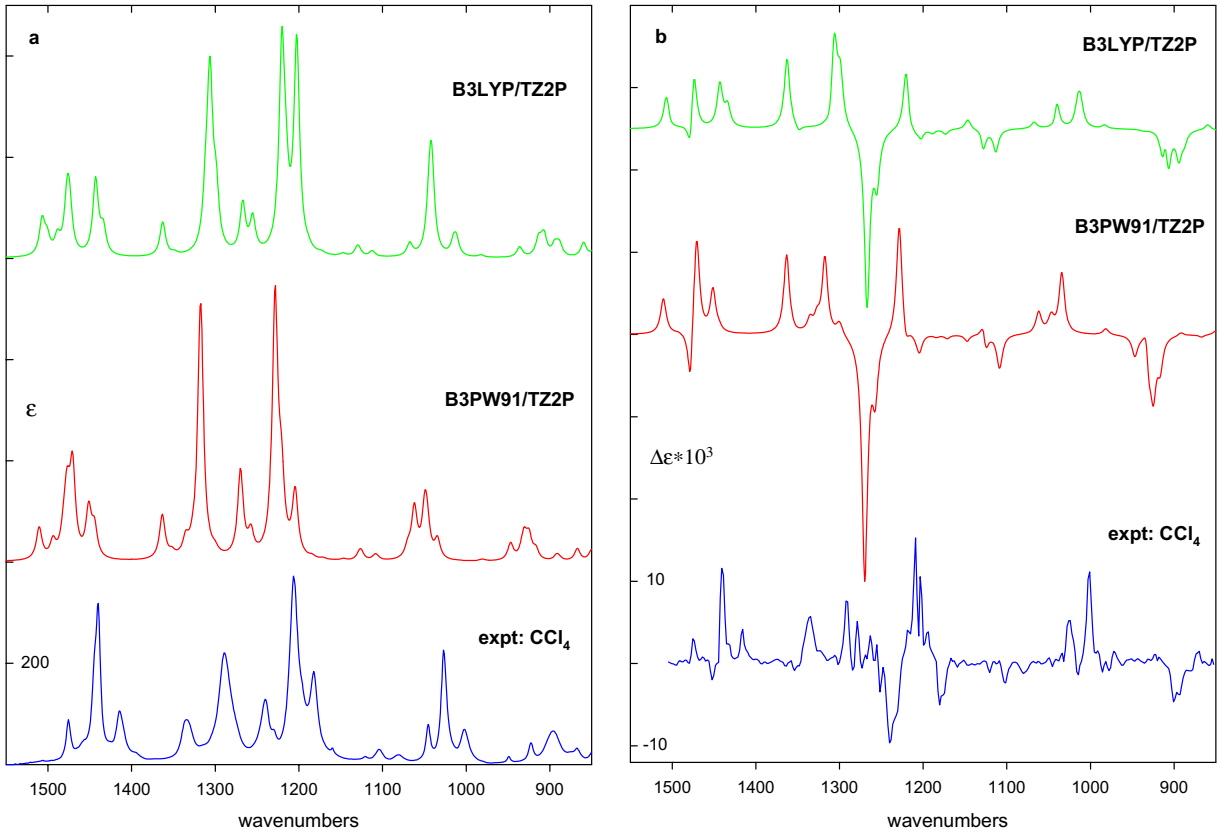

Figure 1. Comparison of B3PW91/TZ2P, B3LYP/TZ2P and experimental IR (**a**) and VCD (**b**) spectra of **1**. The conformationally averaged calculated spectra were obtained using equilibrium populations calculated from relative free energies (Table 3). The experimental spectra are of a 0.22 M solution of (+)-**1** in CCl_4. IR: path length 239μ. VCD: path lengths 597μ (1504–1448 cm^{-1}, 1429–1362 cm^{-1}, 1327–1298 cm^{-1} and 1167–920 cm^{-1}), 239μ (1186–1169 cm^{-1} and 918–852 cm^{-1}) and 109μ (1445–1431 cm^{-1}, 1360–1329 cm^{-1} and 1296–1192 cm^{-1}).

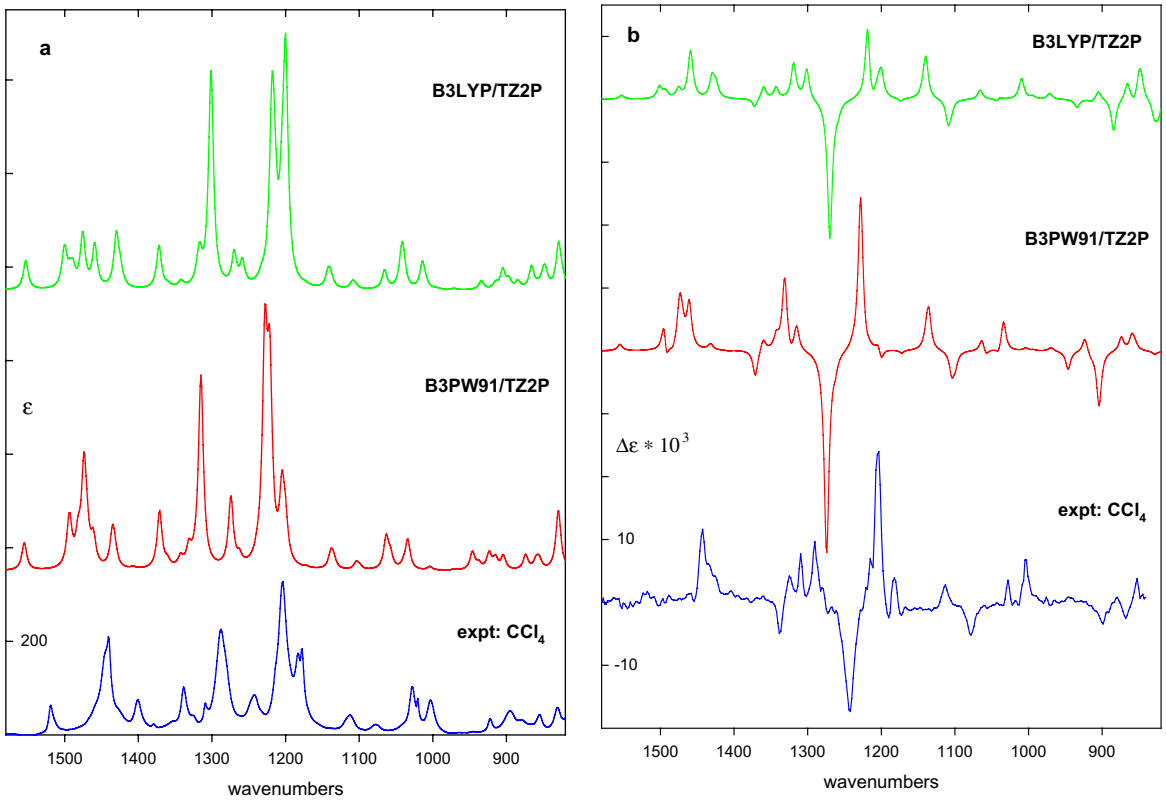

Figure 2. Comparison of B3PW91/TZ2P, B3LYP/TZ2P and experimental IR (**a**) and VCD (**b**) spectra of **2**. The conformationally averaged calculated spectra were obtained using equilibrium populations calculated from relative free energies (Table 3). The experimental spectra are of a 0.23 M solution of (+)-**2** in CCl_4. IR: path length 239μ. VCD: path lengths 597μ (1167–841 cm^{-1}), 239μ (1600–1184 cm^{-1}) and 109μ (1182–1169 cm^{-1}).

The planar $COOCH_3$ and substituted-phenyl moieties of **1**–**3** can rotate about the C2–C7 and C3–C4 bonds linking them to the oxirane ring and, as a result, multiple stable conformations are possible. In order to define the number, structures and relative energies of the stable conformations of **1**–**3**, their potential energy surfaces have been scanned using DFT at the B3LYP/6-31G* level with respect to the dihedral angles O8C7C2H6 and C9C4C3H5. The $COOCH_3$ moiety was *cis*; the *trans*-$COOCH_3$ conformation was substantially higher in energy[12] and has not been considered here. The results are shown in Figure 4 and demonstrate that in **1** and **3** there are four stable conformations, while in **2** there are only two. In all cases, the planar $COOCH_3$ group is approximately perpendicular to the oxirane ring, with the C=O group oriented either towards or away from the oxirane ring. The phenyl rings of **1** and **3** likewise exhibit two stable conformations, interconverted by ~180° rotations about the C3–C4 bond. In the case of **2**, the *para*-substituted phenyl ring exhibits only one inequivalent conformation. Optimization of these stable conformations has been carried out at the TZ2P basis set level using the B3LYP and B3PW91 functionals. The dihedral angles O8C7C2H6 and C9C4C3H5 and the relative energies of the equilibrium geometries obtained are given in Tables 2 and 3, respectively. In the case of **1**, conformations **a** and **b** are close in energy, while **c** and **d** are more than 4 kcal/mol higher. In **a** and **b**, the Br-to-oxirane-O distances are ~4.6 Å, while in **c** and **d** they are ~3.2 Å. The significantly higher energies of **c** and **d** can be attributed to the greater electrostatic repulsion of the Br and O atoms, resulting from their greater proximity. In **a** and **b**, the $COOCH_3$ C=O group is oriented towards and away from the oxirane ring, respectively. In the case of **3**, F-to-oxirane-O distances are >5 Å and the four conformations lie much closer in energy, spanning a range of <0.5 kcal/mol. In the lowest energy conformation, **a**, the $COOCH_3$ C=O group is oriented towards the oxirane ring. In the case of **2**, the $COOCH_3$ C=O group is also oriented towards the oxirane ring in the lowest energy conformation, **a**. Harmonic vibrational frequency calculations confirm that all conformations obtained are stable, and permit their relative free energies, given in Table 3, to be obtained. Relative free energies do not differ greatly from relative energies. Equilibrium populations at room temperature calculated from relative free energies using Boltzmann statistics are also given in Table 3. In the cases of **1** and **2**, two conformations are significantly populated. In the case of **3**, all four conformations are significantly populated. The B3PW91/TZ2P structures of conformations **1a** and **1b**, **2a** and **2b**, and **3a**, **3b**, **3c** and **3d** are shown in Figure 5.

The harmonic vibrational frequencies, dipole strengths and rotational strengths of **1a**, **1b**, **2a**, **2b**, **3a**, **3b**, **3c** and **3d** were calculated at the B3LYP/TZ2P and B3PW91/TZ2P levels. The IR and VCD spectra

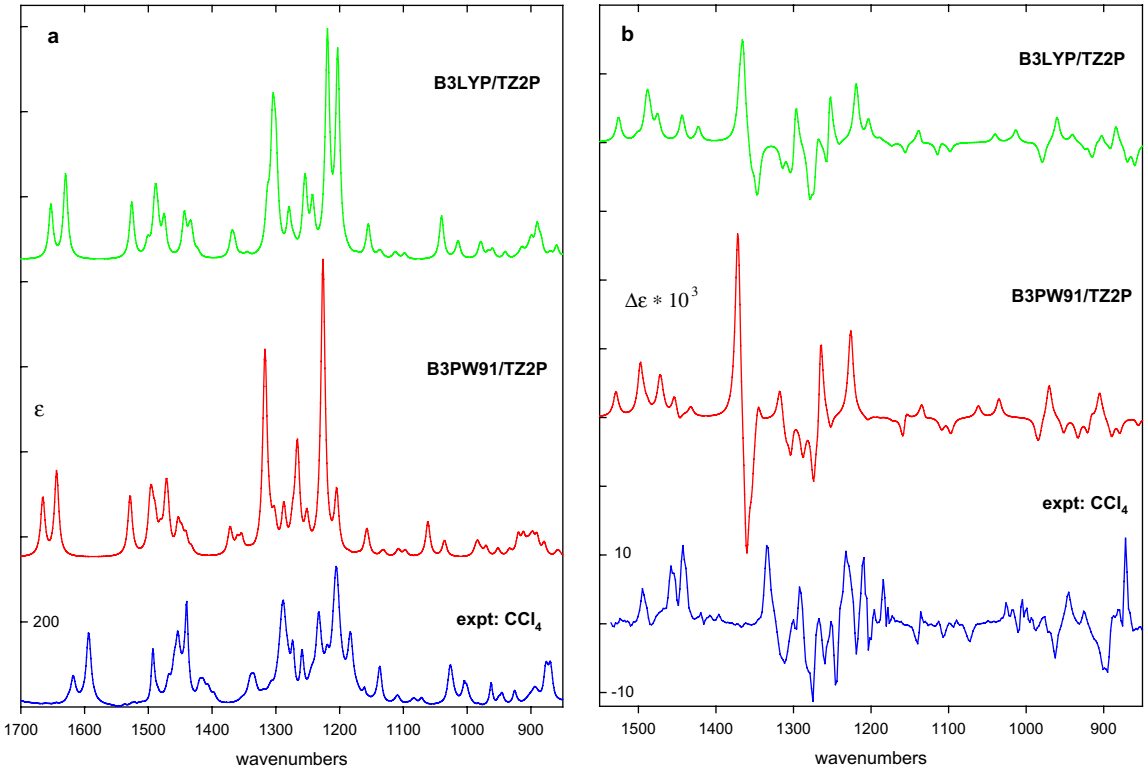

Figure 3. Comparison of B3PW91/TZ2P, B3LYP/TZ2P and experimental IR (**a**) and VCD (**b**) spectra of **3**. The conformationally averaged calculated spectra were obtained using equilibrium populations calculated from relative free energies (Table 3). The experimental IR and VCD spectra are of 0.23 M solutions of (±)-**3** and (+)-**3** in CCl_4, respectively. IR: path length 239μ. VCD: path lengths 597μ (1539–1464 cm^{-1}, 1433–1307 cm^{-1} and 1178–831 cm^{-1}), 239μ (1585–1541 cm^{-1}, 1462–1435 cm^{-1}, 1306–1238 cm^{-1} and 1203–1180 cm^{-1}) and 109μ (1236–1205 cm^{-1}).

obtained thence, together with the conformationally averaged spectra, are shown in Figures 1–3, together with the experimental spectra. Comparison of the conformationally averaged B3LYP/TZ2P and B3PW91/TZ2P IR and VCD spectra of **1**–**3** to the experimental spectra shows that agreement between theory and experiment is somewhat better with the B3PW91 functional. Accordingly, detailed analysis is based on the B3PW91/TZ2P calculations.

In Figure 6, the IR and VCD spectra of equilibrium populations of **1a** and **1b** and the conformationally averaged spectra of **1** are shown for fundamentals 31–45 and compared to the experimental spectra over the range 950–1400 cm^{-1}. The agreement of calculated and experimental IR spectra is excellent, permitting straightforward assignment of the experimental spectrum as detailed in Figure 6A and Table 4. The calculated IR spectra of **1a** and **1b** are very different; in particular, for a substantial number of fundamentals, frequencies differ substantially and, as a result, conformational splittings are observable. Thus, modes 31, 36, 39–42 and 45 of **1a** and modes 32, 41 and 43 of **1b** are clearly resolved. The agreement of the calculated and experimental VCD spectra is less good than for the IR spectra, due to the much lower signal-to-noise ratio of the VCD spectrum. However, VCD arising from modes 31, 36, 39, 41, 42 and 45 of **1a** and modes 31, 34, 41 and 43 of **1b** are observed; the assignment of the experimental spectrum is detailed in Figure 6B and Table 4. The calculated VCD spectrum is for the (2*S*,3*R*)-absolute configuration. It follows that the absolute configuration of **1** is (2*S*,3*R*)-(+)/(2*R*,3*S*)-(−).

Support for the assignment of the IR and VCD spectra of **1** is provided by the comparison of calculated and experimental frequencies, dipole strengths and rotational strengths. Experimental parameters obtained via Lorentzian fitting[20,21] are given in Table 4. As shown in Figure 7, calculated frequencies are 1–4% higher than experimental frequencies; the majority of this difference is attributable to anharmonicity.[23] The agreement of calculated dipole and rotational strengths with the experimental parameters is typical for calculations at this level,[9–15,18–21] providing strong support for the reliability of the structures of the conformations of **1**, for the assignment of the IR and VCD spectra, and for the absolute configuration of **1** derived from the VCD spectrum. Since calculated dipole and rotational strengths are a sensitive function of relative conformational free energies, the excellent agreement with experimental values further demonstrates that the calculated relative free energies must be close to the experimental values.

In Figure 8, the IR/VCD spectra of equilibrium populations of **2a** and **2b** and the conformationally averaged spectra of **2** are shown for fundamentals 33–57/33–48 and compared to the experimental spectra over the ranges 950–1550/950–1350 cm^{-1}. The agreement of cal-

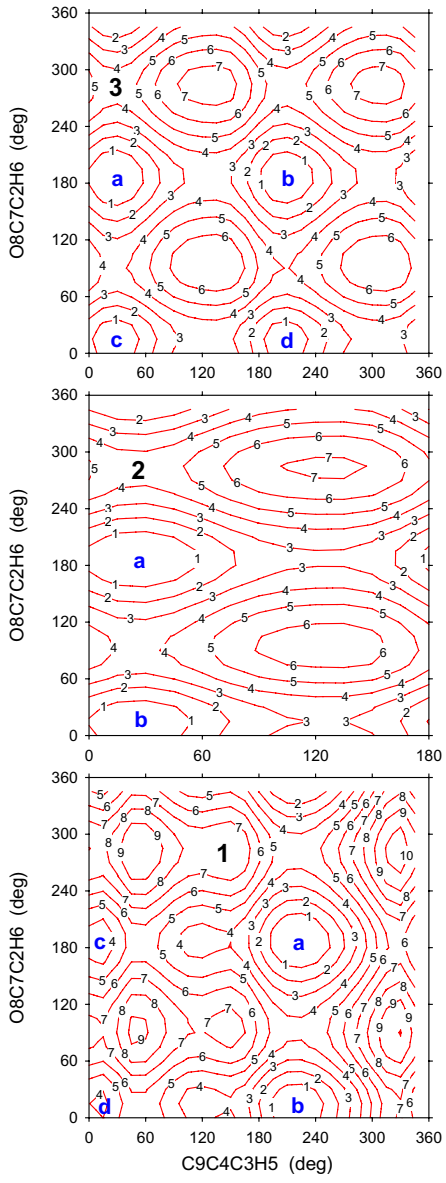

Figure 4. B3LYP/6-31G* potential energy surfaces of (2*S*,3*R*)-**1**, -**2** and -**3**. Dihedral angles were varied in 15° increments. Contour spacing is 1 kcal/mol.

Table 2. TZ2P dihedral angles of the conformations of **1**, **2** and **3**

	O8C7C2H6[a]		C9C4C3H5[a]	
	B3LYP	B3PW91	B3LYP	B3PW91
1a	−170.2	−169.5	43.7	42.7
1b	12.9	13.7	41.3	40.5
1c	−171.9		−169.5	
1d	16.1		−168.7	
2a	−171.1	−170.7	23.6	23.7
2b	15.0	15.9	23.3	23.5
3a	−172.4	−171.5	−154.8	−154.4
3b	−172.2	−171.3	26.3	26.7
3c	14.8	15.6	−154.5	−154.3
3d	14.6	15.7	26.5	26.8

[a] Angles are in degrees. Absolute configuration is (2*S*,3*R*).

culated and experimental IR spectra is excellent, leading straightforwardly to the assignment detailed in Figure 8A

Table 3. TZ2P relative energies, relative free energies and populations of the conformations of **1**, **2** and **3**

	ΔE[a]		ΔG[a]		P (%)[b]	
	B3LYP	B3PW91	B3LYP	B3PW91	B3LYP	B3PW91
1a	0.00	0.00	0.00	0.00	58.5	58.8
1b	0.25	0.26	0.20	0.21	41.5	41.2
1c	4.36		4.57		0.0	
1d	4.80		4.95		0.0	
2a	0.00	0.00	0.00	0.00	63.1	70.5
2b	0.24	0.26	0.31	0.51	36.9	29.5
3a	0.00	0.00	0.00	0.00	33.0	34.2
3b	0.15	0.15	0.08	0.10	28.6	28.9
3c	0.32	0.33	0.28	0.31	20.4	20.0
3d	0.44	0.46	0.36	0.41	17.9	16.9

[a] ΔE and ΔG are in kcal/mole.
[b] Populations are based on ΔG values; $T = 293$ K.

and Table 5. Modes 33, 40–43, 45, 46, 48 and 52 of **2a** and modes 34–36, 45 and 48 of **2b** are clearly identifiable. The agreement of the calculated and experimental VCD spectra is also excellent and the bands with observable VCD intensities are easily assigned. Modes 33, 37/38, 43, 45, 46 and 48 of **2a** and modes 35, 36, 45 and 48 of **2b** are clearly identifiable. The calculated VCD spectrum is for the (2*S*,3*R*)-absolute configuration. It follows that the absolute configuration of **2** is (2*S*,3*R*)-(+)/(2*R*,3*S*)-(−).

The experimental frequencies, dipole strengths and rotational strengths obtained by the Lorentzian fitting are given in Table 5 and compared to the calculated values in Figure 7. The overall agreement of calculated and experimental parameters is comparable to that for **1**, thus further supporting the reliability of the conformational analysis of **2** and of the absolute configuration derived from the VCD spectrum. It should be noted that for modes 42 and 43 of **2a**, the dipole strengths are poorly predicted. For these modes, the predictions of the B3PW91 and B3LYP functionals are substantially different.

In Figure 9, the IR/VCD spectra of equilibrium populations of **3a**, **3b**, **3c** and **3d** and the conformationally averaged spectra of **3** are shown for fundamentals 24–53/24–51 and compared to the experimental spectra over the ranges 850–1700/850–1550 cm^{-1}. Despite the much greater complexity of the IR spectrum of **3** due to the contributions of four conformations, as opposed to two, the agreement of the calculated and experimental IR spectra is remarkably good, leading straightforwardly to the assignment shown in Figure 9A. The greater density of transitions makes it more difficult to identify transitions of individual conformations in the experimental spectrum. Allowing for the less-than-ideal signal-to-noise ratio of the experimental VCD spectrum, the agreement of calculated and experimental spectra is reasonably good and a substantial fraction of the experimental bands observed can be assigned, as shown in Figure 9B. The calculated VCD spectrum is for the (2*S*,3*R*)-absolute configuration. It follows that the absolute configuration of **3** is (2*S*,3*R*)-(+)/2*R*,3*S*-(−).

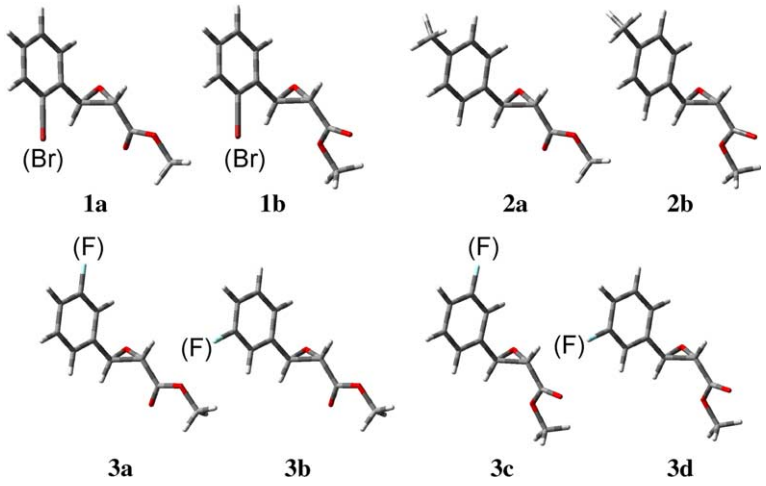

Figure 5. B3PW91/TZ2P geometries for the (2*S*,3*R*) absolute configurations of **1a**, **1b**, **2a**, **2b** and **3a**–**3d**.

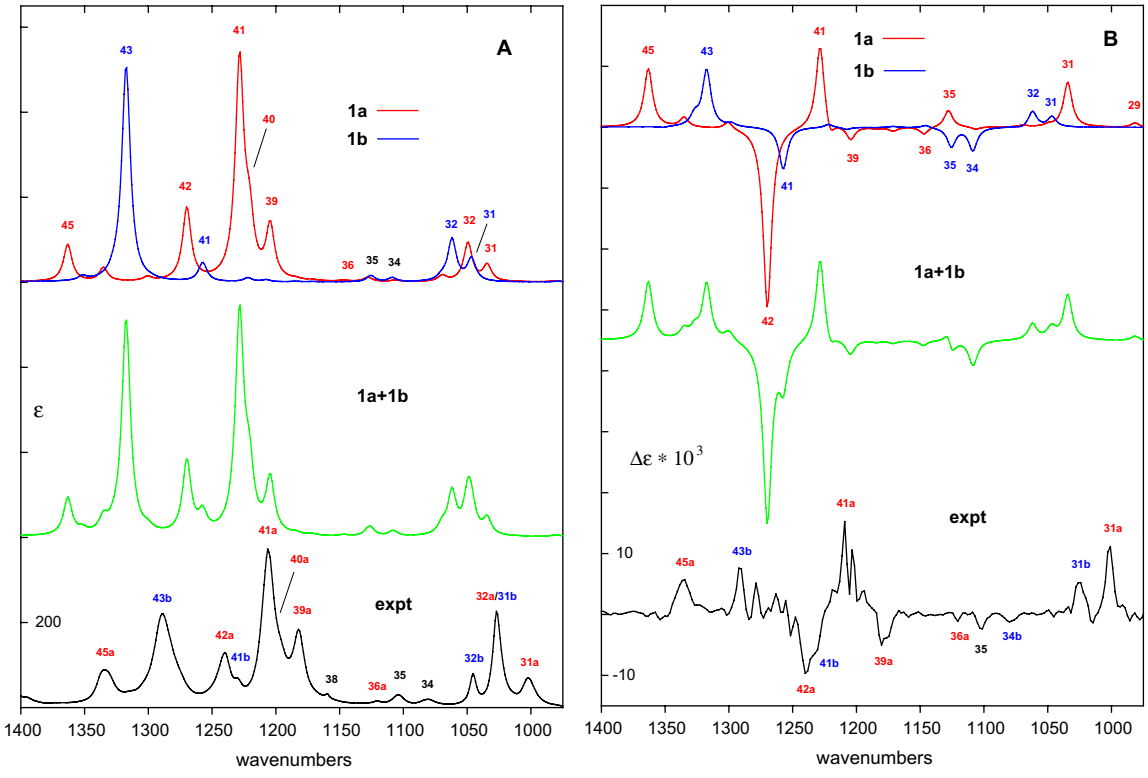

Figure 6. (**A**) Comparison of the conformationally averaged B3PW91/TZ2P IR spectrum of **1** (green) to the experimental IR spectrum of (+)-**1** (black) (from Fig. 1a). The population-weighted B3PW91/TZ2P IR spectra for each conformer **1a** (red) and **1b** (blue) are also shown. (**B**) Comparison of the conformationally averaged B3PW91/TZ2P VCD spectrum of (2*S*,3*R*)-**1** (green) to the experimental VCD spectrum of (+)-**1** (black) (from Fig. 1b). The population-weighted B3PW91/TZ2P VCD spectra for each conformer **1a** (red) and **1b** (blue) are also shown. Fundamentals are numbered. Bands attributable to a single conformation of **1** are highlighted.

Due to the much greater density of transitions in **3**, we have not attempted a Lorentzian deconvolution of its experimental IR and VCD spectra.

4. Discussion

Determination of the absolute configurations of **1**–**3** follows the protocol employed in previous studies.[9–15] First, the PES is scanned at the B3LYP/6-31G* level to determine the number of stable conformations of each molecule. In **1**–**3**, PES scans show that the planar $COOCH_3$ moiety is oriented approximately perpendicularly to the oxirane ring, and the substituted phenyl moieties are oriented in 'tilted' orientations. In **1** and **3**, since there are two inequivalent orientations of both the $COOCH_3$ and substituted phenyl groups, there result four inequivalent, stable conformations. In **2**, only one inequivalent orientation of the *p*-CH_3 substituted phenyl ring exists and there are only two stable conformations.

Table 4. Calculated and experimental frequencies, dipole strengths and rotational strengths for **1**[a]

Mode	Calc[b]						Expt[c]		
	1a			**1b**					
	v	*D*	*R*	*v*	*D*	*R*	*v*	*D*	*R*
45	1363	125.2	34.6	1352	21.1	−1.0	1334	122.4	18.6
44	1335	46.4	5.8	1327	19.7	9.0	1299	25.3	
43				1317	1081.1	49.7	1289	323.3	14.8
	1301	13.9	4.6				1277	56.4	
42				1298	3.5	2.6			
	1270	263.9	−114.7				1241	142.0	−30.7
41				1257	99.4	−38.4	1230	23.2	−8.3
	1228	819.5	55.7				1206	432.9	27.7
40	1221	197.3	−10.8	1222	21.3	3.1	1197	89.3	13.0
39	1204	202.8	−8.8	1208	11.2	−2.1	1182	211.0	−13.9
38	1184	4.9	−0.9	1184	3.7	−0.3	1159	17.5	
37	1171	3.2	−2.6	1171	2.5	1.0			
36	1147	4.7	−5.1	1146	0.5	2.6	1121	16.0	−1.4
35	1128	17.6	12.1	1125	36.9	−19.7	1104	36.0	−5.1
34	1106	6.3	−1.8	1109	24.1	−23.9	1081	22.0	−3.6
33	1069	24.7	1.3	1070	21.6	−1.8			
32				1062	262.7	17.1	1045	66.3	
	1049	170.4	1.5				1027	187.4	
31				1047	142.5	11.3	1022	37.6	12.7
	1034	72.5	35.1				1002	105.2	27.3

[a] Frequencies in cm^{-1}; dipole strengths in 10^{-40} esu^2cm^2; rotational strengths in 10^{-44} esu^2cm^2.
[b] B3PW91/TZ2P.
[c] From Lorentzian fitting.

Equilibrium geometries, relative energies, relative free energies and percentage populations (at room temperature) have been calculated for the stable conformations of **1**–**3**, using both B3LYP and B3PW91 functionals and at the TZ2P basis set level. The TZ2P basis set is used because this is the basis set of choice for the subsequent calculations of IR and VCD spectra. In **2** and **3**, all stable conformations are close in energy and free energy and, as a result, are predicted to be substantially populated at room temperature. In **1**, a large gap (over 4 kcal/mol) occurs between conformations **a**/**b** and **c**/**d**, due to greater Br···O repulsion in the latter; as a result only two of the four conformations are substantially populated.

The IR and VCD spectra of **1**–**3** are then predicted. As in prior studies,[9–15] we focus on the mid-IR spectral region. IR and VCD spectra of each conformation are calculated at the B3LYP/TZ2P and B3PW91/TZ2P levels, the use of two functionals providing a gauge of the sensitivity of predicted spectra to the choice of functional. Conformationally averaged spectra are then obtained, using the populations calculated from relative ΔG values. The calculated IR spectra of **1** and **2** are in good agreement with the experimental spectra, the B3PW91 spectra being in better agreement than the B3LYP spectra. Using the B3PW91/TZ2P spectra, we can then make detailed assignments of the experimental IR spectra of **1** and **2**. Since the two conformations, **a** and **b**, exhibit very different spectra, for both **1** and **2** we can identify bands in the experimental spectra originating in individual conformations. This provides very strong support for the reliability of the predicted structures of the conformations **a** and **b**. Furthermore, since the intensities of the experimental spectra are well reproduced by the calculated spectra, we can conclude that the relative free energies and populations of **a** and **b** are also reliably predicted. Having assigned the IR spectra of **1** and **2** unambiguously, we then compare predicted and experimental VCD intensities, and determine for which absolute configuration the calculated VCD intensities match the experimental VCD intensities with respect to sign. In principle, one band suffices; however, greater reliability is obtained by using multiple bands. In both **1** and **2**, the VCD of ~10 bands is unambiguously detectable. In every case, for both **1** and **2** agreement of calculated and experimental signs is found when the spectra of the (2*S*,3*R*)-absolute configurations and the (+)-isomers are compared. Thus, for **1** and **2**, the absolute configurations are unambiguously (2*S*,3*R*)-(+)/(2*R*,3*S*)-(−). The quantitative agreement of calculated and experimental VCD intensities is also excellent, further supporting the reliability of the analysis. In the case of **3**, the significant population of the four conformations results in much more dense IR and VCD spectra. As a result, detailed assignment of the experimental spectra is substantially more difficult.

We have previously reported TDDFT calculations of the $[\alpha]_D$ values of **1**–**3** and in each case predicted a positive rotation for the (2*S*,3*R*)-absolute configuration. The VCD studies reported herein confirm the absolute configurations obtained from the $[\alpha]_D$ calculations. This is of importance since the VCD methodology provides much more reliable absolute configurations than does the calculation of $[\alpha]_D$ values. The case of **1** is an excellent illustration of this. The $[\alpha]_D$ values of conformations

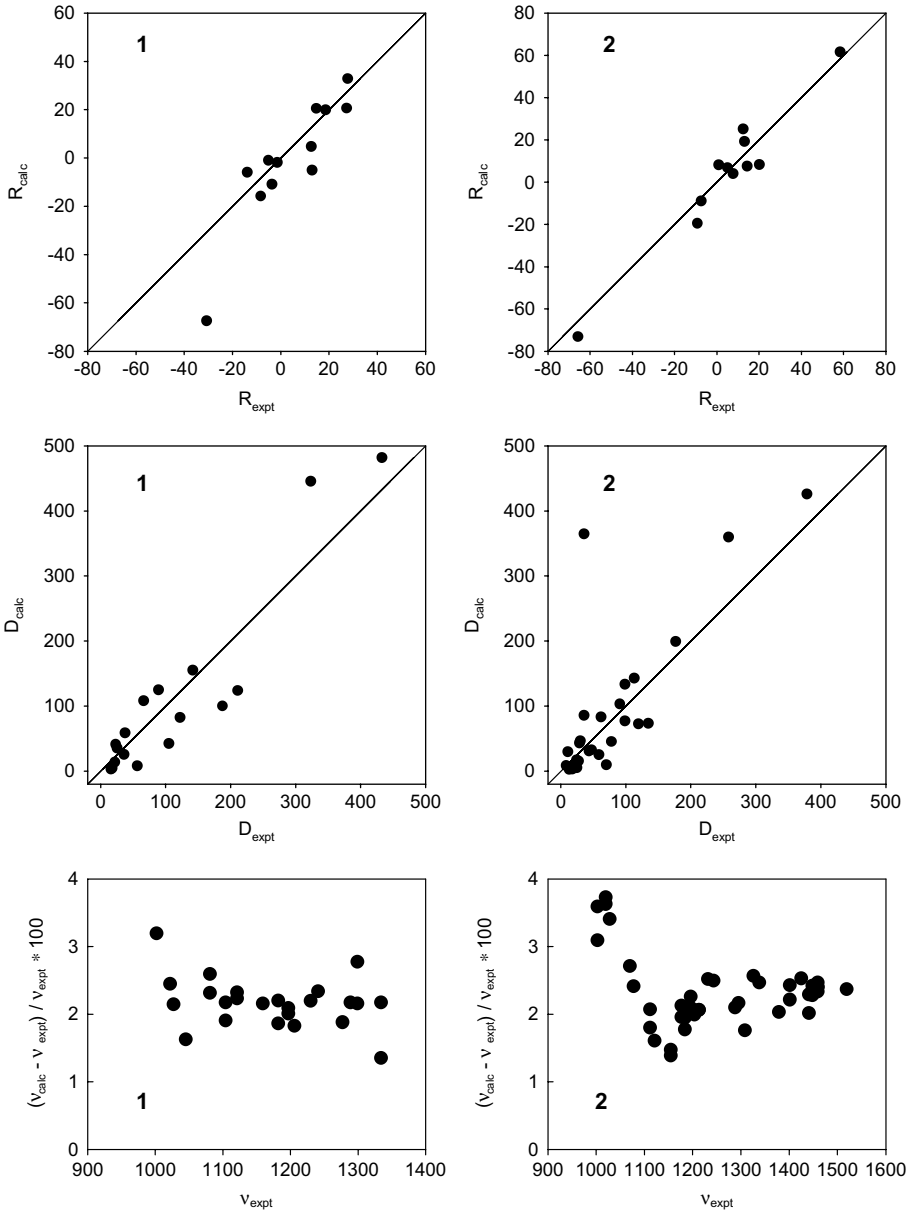

Figure 7. Comparison of the B3PW91/TZ2P calculated frequencies (in cm^{-1}), dipole strengths (in 10^{-40} esu^2 cm^2) and rotational strengths (in 10^{-44} esu^2 cm^2) to their experimental values for **1** and **2**.

a and **b** are relatively small and opposite in sign (Table 6). The conformationally averaged $[\alpha]_D$ value for (2*S*,3*R*)-**1** is positive when the calculated conformational free energy difference is used to calculate the populations of **a** and **b**. However, calculated $[\alpha]_D$ values are not exact: extensive studies have shown that for conformationally rigid molecules with $[\alpha]_D$ values $\leqslant 100$ the RMS error is ~ 30.[7] The calculated ΔG value is also not exact; errors of a few tenths of a kcal/mol can significantly change calculated conformational populations and, hence, conformationally averaged $[\alpha]_D$ values.[6] Thus, the error in $[\alpha]_D$ for **a** and **b** together with the error in ΔG could result in an erroneous prediction of the sign of $[\alpha]_D$. Analysis of the IR and VCD spectra of **1** does not suffer from this ambiguity. The predicted structures and relative free energies of conformations **a** and **b** are validated by the comparison of predicted and experimental IR spectra. The assignment of the IR spectrum of **1** definitively proves the existence of conformations **a** and **b**. The quantitative comparison of calculated and experimental dipole and rotational strengths verifies the reliability of the predicted structures, IR spectra and relative free energies of **a** and **b**. As a result, the analysis of the VCD spectrum does not suffer from any uncertainty in regard to the conformational analysis of **1**. The absolute configuration of **1** follows directly from the comparison of calculated and experimental rotational strengths. If the absolute configuration is (2*S*,3*R*)-(+) the agreement is excellent; the signs of all VCD bands are correctly predicted. If the absolute configurations were (2*S*,3*R*)-(−), the calculated and experimental rotational strengths would be in perfect disagreement. Thus, unambiguously, the absolute configuration is (2*S*,3*R*)-(+).

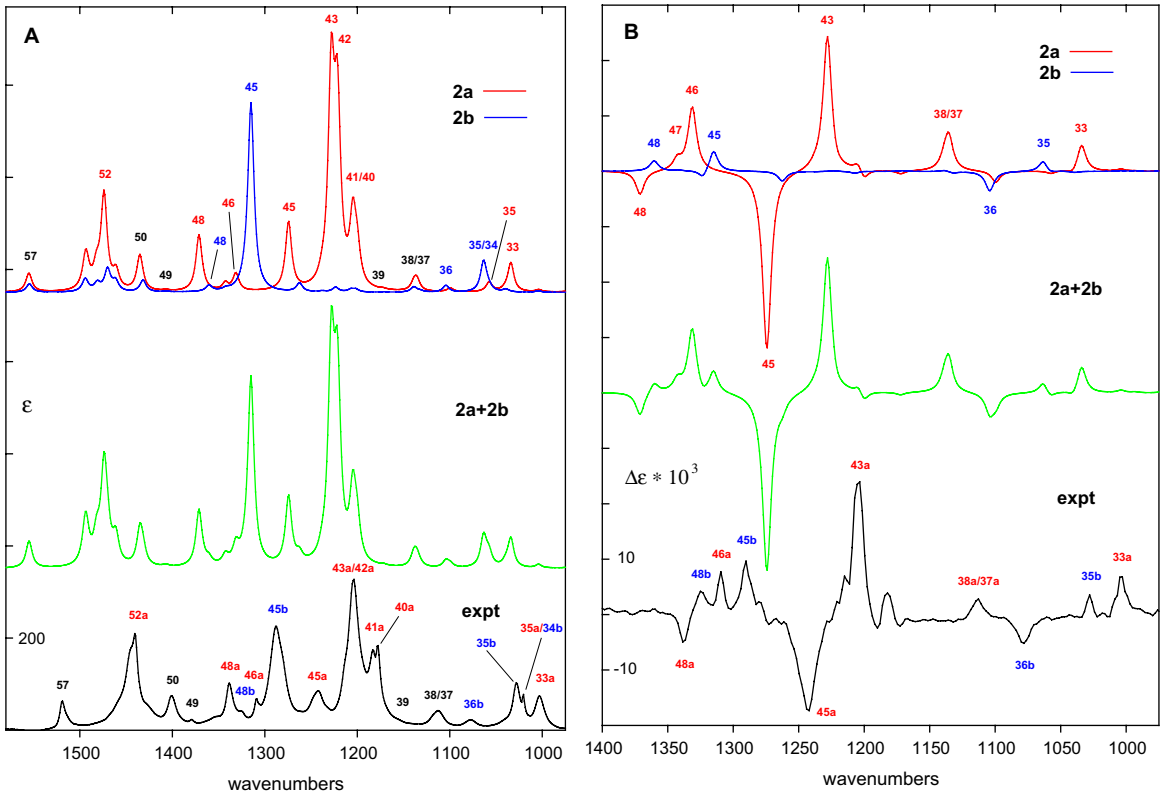

Figure 8. (**A**) Comparison of the conformationally averaged B3PW91/TZ2P IR spectrum of **2** (green) to the experimental IR spectrum of (+)-**2** (black) (from Fig. 2a). The population-weighted B3PW91/TZ2P IR spectra for each conformer **2a** (red) and **2b** (blue) are also shown. (**B**) Comparison of the conformationally averaged B3PW91/TZ2P VCD spectrum of (2*S*,3*R*)-**2** (green) to the experimental VCD spectrum of (+)-**2** (black) (from Fig. 2b). The population-weighted B3PW91/TZ2P VCD spectra for each conformer **2a** (red) and **2b** (blue) are also shown. Fundamentals are numbered. Bands attributable to a single conformation of **2** are highlighted.

Table 5. Calculated and experimental frequencies, dipole strengths and rotational strengths for **2**[a]

Mode	Calc[b]						Expt[c]		
	2a			**2b**					
	ν	*D*	*R*	*ν*	*D*	*R*	*ν*	*D*	*R*
57	1555	42.5	2.2	1555	45.5	1.1	1519	28.9	
56	1495	21.3	25.0	1494	39.0	−51.2	1459	35.7	
55	1493	69.2	−27.8	1494	34.6	69.5			
54	1483	18.4	−3.6	1482	19.4	1.4	1448	77.8	
53	1482	27.2	0.9	1481	26.0	−0.3			
52	1474	229.1	20.5	1470	127.7	15.7	1441	176.8	
51	1461	41.6	16.7	1461	57.6	7.8	1425	30.0	
50	1435	88.9	0.4	1432	69.3	5.9	1401	61.9	
49	1407	2.9	−0.1	1407	4.0	−0.4	1379	17.8	
48	1371	146.5	−12.6				1338	90.7	−7.4
				1360	37.6	13.4	1326	21.8	7.7
47	1343	19.6	5.8	1342	12.6	1.2			
46	1331	46.4	35.6				1308	47.1	12.5
				1323	17.6	−11.0	1295	24.7	
45				1315	1220.1	28.3	1288	257.9	20.1
	1274	189.7	−103.7				1243	98.7	−65.7
44				1263	57.6	−13.5	1232	24.2	
	1238	11.0	1.5				1213	70.2	8.1
43				1238	6.2	−0.4			
	1228	604.4	82.8				1204	378.6	61.6
42	1221	503.7	−4.5	1223	32.7	1.1	1196	35.9	
41	1205	195.4	4.8	1207	17.4	−2.9	1184	113.3	

(*continued on next page*)

Table 5 (*continued*)

Mode	Calc[b]						Expt[c]		
	2a			**2b**					
	v	*D*	*R*	*v*	*D*	*R*	*v*	*D*	*R*
40	1200	95.9	−6.4	1202	19.2	0.4	1177	134.9	
39	1172	2.9	−2.0	1171	2.5	0.9	1155	12.8	
38	1139	25.8	6.5	1139	39.5	2.1	1121	10.7	
37	1135	31.8	21.4	1132	9.6	−2.4	1112	58.6	7.5
36				1104	51.5	−31.2	1078	27.4	−19.5
	1099	11.9	−7.6				1070	8.1	
35				1063	246.6	17.4	1028	119.7	6.8
	1057	31.9	−1.8						
								1020	43.4
34				1058	28.7	−4.5			
	1041	3.5	−3.5						
33	1034	100.0	19.4	1039	22.2	−2.0	1003	98.6	19.2

[a] Frequencies in cm^{-1}; dipole strengths in 10^{-40} esu^2cm^2; rotational strengths in 10^{-44} esu^2cm^2.
[b] B3PW91/TZ2P.
[c] From Lorentzian fitting.

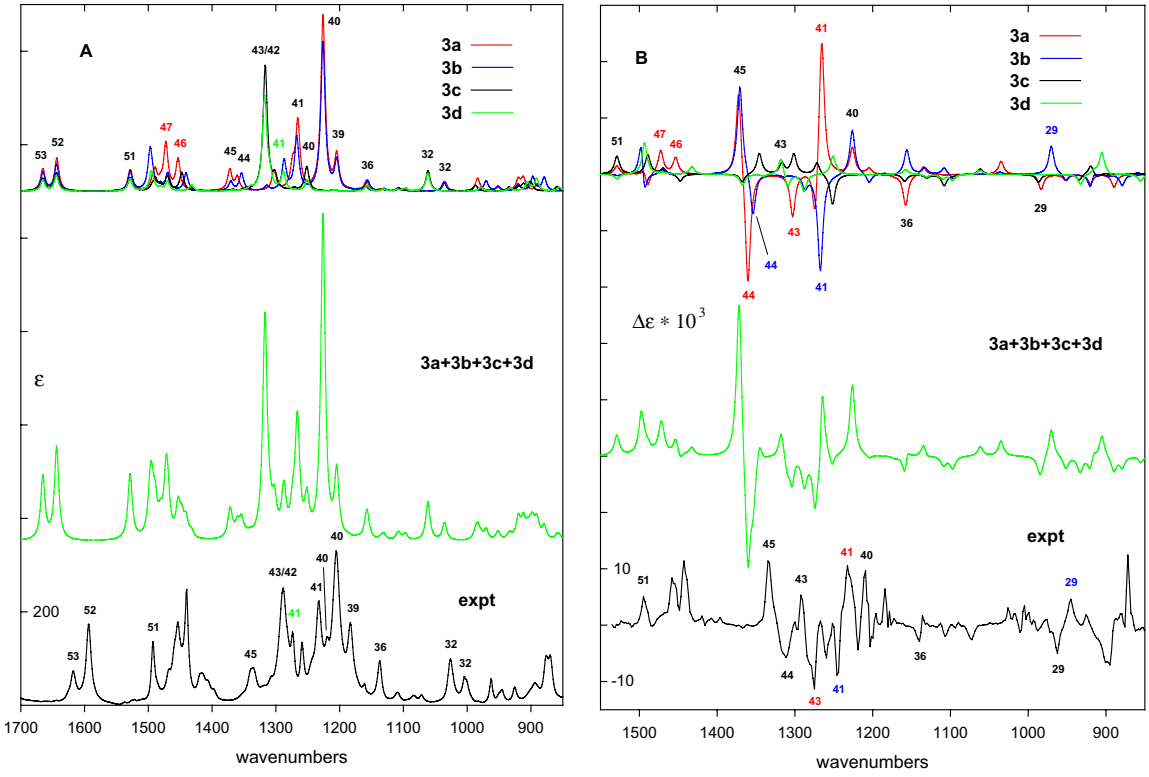

Figure 9. (**A**) Comparison of the conformationally averaged B3PW91/TZ2P IR spectrum of **3** (green) to the experimental IR spectrum of (±)-**3** (black) (from Fig. 3a). The population-weighted B3PW91/TZ2P IR spectra for each conformer **3a** (red), **3b** (blue), **3c** (black) and **3d** (green) are also shown. (**B**) Comparison of the conformationally averaged B3PW91/TZ2P VCD spectrum of (2*S*,3*R*)-**3** (green) to the experimental VCD spectrum of (+)-**3** (black) (from Fig. 3b). The population-weighted B3PW91/TZ2P VCD spectra for each conformer **3a** (red), **3b** (blue), **3c** (black) and **3d** (green) are also shown.

In the cases of **2** and **3**, there is less uncertainty in the absolute configurations determined from $[\alpha]_D$ values. The $[\alpha]_D$ values of all conformations of (2*S*,3*R*)-**2** and (2*S*,3*R*)-**3** are positive in sign and >90 in magnitude. Thus, the conformationally averaged $[\alpha]_D$ values are positive for any relative free energy values. In addition, errors in conformational $[\alpha]_D$ values of the expected magnitude would not change this conclusion. Nevertheless, the calculated and experimental $[\alpha]_D$ values are not close in magnitude, leaving some room for doubt regarding their reliability and, hence, that of the absolute configurations predicted. The absolute configura-

Table 6. Calculated and experimental specific rotations of **1**–**3**

	$[\alpha]_D$ (calc)[a] 2*S*,3*R*	$[\alpha]_D$[b] 2*S*,3*R*	$[\alpha]_D$ (expt)[c]
1a	+101.3		
1b	−34.2	+45.1	+23 (*c* 5.6, CCl_4)
1c	+414.3		
1d	+293.7		
2a	+370.7	+293.2	+174 (*c* 4.3, CCl_4)
2b	+160.8		
3a	+340.8		
3b	+283.9	+240.6	+154 (*c* 4.5, CCl_4)
3c	+145.4		
3d	+96.6		

[a] Calculated at the B3LYP/6-31G* geometry using the B3LYP functional and the aug-cc-pVDZ basis set.[6]

[b] Conformational average obtained from populations based on ΔG values given in Table 3.

[c] From Table 1.

tions determined using VCD for **2** and **3** are clearly unambiguous and thus of higher reliability.

The primary products of the asymmetric epoxidations used to synthesize **1**–**3** are the parent carboxylic acids. In order to determine their absolute configurations, we have made use of their methyl esters. At the concentrations used for VCD measurements, *mono*-carboxylic acids are substantially dimerized and the analysis of their spectra requires calculations for an equilibrium mixture of monomer and dimer species.[24] The use of the methyl esters eliminates aggregation and permits experimental spectra to be compared to spectra calculated for monomeric forms of the molecules of interest. In the case of **1**–**3**, the signs of $[\alpha]_D$ are the same as those of the precursor acids. It follows that the absolute configurations of the parent carboxylic acids are also uniformly (2*S*,3*R*)-(+)/(2*R*,3*S*)-(−).

It has previously been shown that the absolute configurations of *trans*-phenyl glycidic acid and its methyl ester are (2*S*,3*R*)-(+).[4] We have therefore shown that the *o*-Br, *p*-Me and *m*-F substitutions in **1**, **2** and **3** do not lead to changes in the absolute configuration.

Our results define the absolute stereochemistries of the asymmetric epoxidations of *o*-Br-, *p*-Me- and *m*-F-*trans*-cinnamic acid using keto bile acids and Oxone. The mechanism of these asymmetric epoxidation reactions has been discussed by Bortolini et al.[2] and the asymmetric epoxidation of olefins using chiral dioxanes has recently been reviewed.[25,26] Asymmetric epoxidation of olefins using chiral dioxiranes. Our results enable a more critical evaluation of the proposed mechanism to be made. Ab initio calculations are in progress to predict the absolute stereochemistries of asymmetric epoxidations using a range of keto bile acids and cinnamic acid derivatives and, hence, to determine whether the proposed mechanism is consistent with the observed stereochemical data. Our results will be reported in a future publication.

Acknowledgements

We are grateful to the National Science Foundation for support of this work via grant CHE-0209957, to the USC Center for High Performance Computing and Communications, HPCC, for computer time, and to MURST (Italy) PRIN 2003 for financial support.

References

1. Bortolini, O.; Fogagnolo, M.; Fantin, G.; Maietti, S.; Medici, A. *Tetrahedron: Asymmetry* **2001**, *12*, 1113–1115.
2. Bortolini, O.; Fantin, G.; Fogagnolo, M.; Forlani, R.; Maietti, S.; Pedrini, P. *J. Org. Chem.* **2002**, *67*, 5802–5806.
3. Bortolini, O.; Fantin, G.; Fogagnolo, M.; Mari, L. *Tetrahedron: Asymmetry* **2004**, *15*, 3831–3833.
4. Plucinska, K.; Kasprzykowski, F.; Kozian, E. *Tetrahedron Lett.* **1997**, *38*, 861–864.
5. Stephens, P. J.; Devlin, F. J.; Cheeseman, J. R.; Frisch, M. J. *J. Phys. Chem. A* **2001**, *105*, 5356–5371.
6. Stephens, P. J.; Devlin, F. J.; Cheeseman, J. R.; Frisch, M. J.; Bortolini, O.; Besse, P. *Chirality* **2003**, *15*, S57–S64.
7. Stephens, P. J.; McCann, D. M.; Cheeseman, J. R.; Frisch, M. J. *Chirality* **2005**, *17*, S52–S64.
8. Stephens, P. J.; Devlin, F. J. *Chirality* **2000**, *12*, 172–179.
9. Stephens, P. J.; Aamouche, A.; Devlin, F. J.; Superchi, S.; Donnoli, M. I.; Rosini, C. *J. Org. Chem.* **2001**, *66*, 3671–3677.
10. Devlin, F. J.; Stephens, P. J.; Scafato, P.; Superchi, S.; Rosini, C. *Tetrahedron: Asymmetry* **2001**, *12*, 1551–1558.
11. Devlin, F. J.; Stephens, P. J.; Scafato, P.; Superchi, S.; Rosini, C. *Chirality* **2002**, *14*, 400–406.
12. Devlin, F. J.; Stephens, P. J.; Oesterle, C.; Wiberg, K. B.; Cheeseman, J. R.; Frisch, M. J. *J. Org. Chem.* **2002**, *67*, 8090–8096.
13. Stephens, P. J. In *Computational Medicinal Chemistry for Drug Discovery*; Bultinck, P., de Winter, H., Langenaecker, W., Tollenaere, J., Eds.; Dekker: New York, 2003, Chapter 26, pp 699–725.
14. Ricci, A.; Devlin, F. J.; Stephens, P. J.; Gasparrini, F.; Rompietti, R.; Villani, C. *J. Org. Chem.* **2005**, *70*, 664–669.
15. Devlin, F. J.; Stephens, P. J.; Besse, P. *Tetrahedron: Asymmetry* **2005**, *16*, 1557–1566.
16. GAUSSIAN 98, Gaussian Inc. www.gaussian.com.
17. Stephens, P. J.; Jalkanen, K. J.; Amos, R. D.; Lazzeretti, P.; Zanasi, R. *J. Phys. Chem.* **1990**, *94*, 1811–1830.
18. Cheeseman, J. R.; Frisch, M. J.; Devlin, F. J.; Stephens, P. J. *Chem. Phys. Lett.* **1996**, *252*, 211–220.
19. Stephens, P. J.; Ashvar, C. S.; Devlin, F. J.; Cheeseman, J. R.; Frisch, M. J. *Mol. Phys.* **1996**, *89*, 579–594.
20. Devlin, F. J.; Stephens, P. J.; Cheeseman, J. R.; Frisch, M. J. *J. Phys. Chem.* **1997**, *101*, 6322–6333.
21. Devlin, F. J.; Stephens, P. J.; Cheeseman, J. R.; Frisch, M. J. *J. Phys. Chem.* **1997**, *101*, 9912–9924.
22. Yang, D.; Wong, M.-K.; Yip, Y.-C. *J. Org. Chem.* **1995**, *60*, 3887–3889.
23. Finley, J. W.; Stephens, P. J. *J. Mol. Str., (Theochem.)* **1995**, *357*, 225–235.
24. Urbanová, M.; Setnička, V.; Devlin, F. J.; Stephens, P. J. *J. Am. Chem. Soc.* **2005**, *127*, 6700–6711.
25. Shi, Y. *Acc. Chem. Res.* **2004**, *37*, 488–496.
26. Yang, D. *Acc. Chem. Res.* **2004**, *37*, 497–505.